Varian Eclipse Stereotactic Cone Data Commissioning

Dominika Firth (dominika.firth@genesiscare.com)
Genesis Care Pty Ltd https://orcid.org/0000-0003-1456-6462
Penny Fogg
Genesis Care Pty Ltd
Peter Christiansen
Genesis Care Pty Ltd

Research Article

Keywords: Stereotactic radiosurgery, conical collimator, Varian TrueBeam, microDiamond, SRS Diode, gamma analysis

Posted Date: April 27th, 2022

DOI: https://doi.org/10.21203/rs.3.rs-1552195/v1

Varian Eclipse Stereotactic Cone Data Commissioning

Dominika Firth, Penny Fogg, Peter Christiansen

Abstract Conical collimators are effective and readily available accessories for the field shaping of small stereotactic fields, however the measurements required to accurately characterise the smallest radiation fields are difficult and prone to large errors. Furthermore, there is little published commissioning data to compare measurements against.

The aim of this investigation was to commission the cone dose calculation algorithm of a Varian Eclipse treatment planning system for a Varian 5mm conical collimator attached to a Varian TrueBeam linear accelerator that had been beam-matched to the Varian Golden Beam Data (GBD). Tissue maximum ratios (TMRs), off-axis ratios (OARs), and the output factor (OF) were measured using a PTW 60019 microDiamond and a PTW 60018 SRS Diode detector. Results were compared to the GBD for this collimator, radiochromic film measurements, and an output factor measured during an independent audit by the Australian Clinical Dosimetry Service. Film dosimetry was used to evaluate Eclipse dose calculations in a solid water phantom and end-to-end accuracy with an anthropomorphic head phantom.

A PTW BEAMSCAN water phantom was used to collect the data, and output correction factors were derived from IAEA TRS-483. Gamma analysis was used to compare measured TMRs and profiles, and to compare Eclipse dose planes with film dosimetry results.

Good agreement was obtained between the measurements with the two detectors, and with the various comparisons carried out to confirm both measurement accuracy and planning system configuration. It was decided to configure Eclipse with the microDiamond OF and the SRS Diode measured TMR and OAR data.

D. Firth, P. Fogg, P. Christiansen
GenesisCare, Buderim, Queensland, Australia
Dominika.firth@genesiscare.com
https://orcid.org/0000-0003-1456-6462

Keywords Stereotactic radiosurgery, conical collimator, Varian TrueBeam, microDiamond, SRS Diode, gamma analysis

Introduction

Stereotactic radiosurgery (SRS) is a radiotherapy technique used to treat small, localised cranial lesions inaccessible by surgery. It involves the very accurate delivery of high radiation doses to the planned target volume while minimising dose to surrounding sensitive cranial structures. Conical collimator accessories define small circular radiation fields for SRS treatments by attaching to the linear accelerator (linac) head with dedicated mounting ensuring very accurate central axis alignment [1]. This investigation focused on the 5mm Varian cone for a TrueBeam linac because of the difficulty of carrying out the required measurements in such a small radiation field.

The main issues when working with small fields (less than 3cm across at isocentre) are the accuracy of the measurements, detector choice, and lack of comparison data for specific combinations of linac, modality and collimation type. Small fields are characterised by three effects; detector volume averaging, lack of charged particle equilibrium and partial occlusion of the primary photon source. The ideal characteristics of a small field detector include small sensitive volume and overall detector size to reduce the dose volume effect, low noise, and near water equivalence to minimise heterogeneity effects. In practice, most commonly available detectors deviate from the ideal. The variation of stopping-power ratios and perturbation factors with field size also becomes significant in these small fields thus requiring field and detector-dependent output correction factors, such as those published in IAEA TRS-483, to be applied to measured small field output factors [2]. Detector type, cone and linac vendor, planning system algorithm requirements, and the application of the output correction factor, therefore all contribute to the variety of available comparison data for cone commissioning.

Table 1 *- Previous approaches, from knowledge available to us, to 5mm cone commissioning output factor measurement.*

Ref	First author surname	Description
3	Cheng	Varian TrueBeam (Edge Diode, SFD and A16) and Monte Carlo
4	Smith	Elekta Versa linac (microDiamond and others)
5	Oliver	Elekta Synergy linac (microDiamond and others)

The aim of this investigation was to measure tissue maximum ratios (TMRs), off-axis ratios (OARs) and output factor (OF) to configure the Cone Dose Calculation (CDC) algorithm V15.6 for the Varian 5mm ICVI cone on a Varian TrueBeam V2.7 linac commissioned to match the Varian Golden Beam Data (GBD) for the Varian Eclipse treatment planning system (TPS). Verification of these measurements was made through comparisons with the GBD, Australian Clinical Dosimetry Service (ACDS) audit results, and radiochromic film dosimetry results. The significance of this investigation includes contribution to the cone commissioning data literature pool providing greater comparison opportunities for others with a similar commissioning task.

Methodology

Beam Data Measurement

The measurement of the OF, TMRs and OARs for the 5mm ICVI conical applicator were completed on a Varian TrueBeam linac with jaw size configured in Eclipse and TrueBeam administration during linac commissioning for all cone sizes to 5.0x5.0cm^2 to match the Varian recommendations as per the GBD jaw setting. All measurements were completed with the gantry at 0^0 and collimator at 90^0 for an accelerator calibrated to deliver 1cGy/MU for a 10x10cm^2 field size at 100cm SSD and depth of dose maximum.

Commissioning data was collected with a PTW 60019 microDiamond detector and a PTW 60018 SRS Diode in a PTW BEAMSCAN water tank phantom V4.2 for a 6MV flattening filter free (FFF) photon beam [6,7].

The microDiamond detector is a suitable choice for small field dosimetry. Overresponse due to mass density effects has been found to be offset to some extent by its volume averaging effect [8]. Importantly, TRS-483 contains correction factor data appropriate for a 5mm circular field OF measured with the PTW 60019 microDiamond. The TRS-483 correction factor for the PTW 60019 microDiamond was obtained for an equivalent square field size of 0.43cm (based on the equivalent area of the measured full-width half-maximum (FWHM)) by fitting the tabulated data to a fourth order polynomial curve for interpolation of the required correction value, found to be 0.957 [2]. The ACDS used an output correction factor of 0.955 for the microDiamond based on the nominal field size.

The PTW 60018 SRS Diode has the advantage of a smaller radius perpendicular to the beam axis than the PTW 60019 microDiamond detector (0.6mm and 1.1mm, respectively), resulting in less volume averaging which is an advantage for the measurement of OARs [6]. The output correction factor for the SRS Diode was

determined similarly to the microDiamond correction factor, found to be 0.947, however this was extrapolated down due to the 5mm minimum published equivalent square field size for the detector [2,6]. An output correction factor from unpublished TRS-483 data for the SRS Diode was applied and adding this data point to the polynomial fit made the equivalent square field size correction factor 0.946.

Varian GBD has been reported as an output ratio for the Edge detector to which an output correction factor was not applied [2,9].

Extreme care was taken to set up the BEAMSCAN water tank phantom accurately given the sensitivity of small field measurements to misalignment. It has been shown that a 1mm displacement in dosimeter position can lead to a 6.3% error in the measured output factor for a 5mm field, reducing to 1% for a 15mm field, which highlights the importance of meticulous equipment setup for very small fields [10]. The inclination angle between the depth scan axis and the collimator rotation axis was evaluated using the in-built beam inclination test and the water tank was manually adjusted with a levelling platform to achieve measured inclination angles no larger than 0.01^0 in the in-plane and cross-plane directions. The results from the beam inclination test were also used to position the detector at the field centre to within 0.1mm.

The OF was measured at 95cm SSD and 5cm depth, normalised to a $10x10cm^2$ reference field under the same conditions. Dose rates of 1000MU/minute and 1400MU/minute were used for these measurements; however, it was found that this had no statistically significant influence on the measured output and these values were averaged for the OF calculation.

TMRs were measured directly and not calculated from percentage depth doses, as recommended for small fields [2,11,12]. TMR scans were performed at 100cm SDD and were repeated to check reproducibility. The step size used for TMR measurement was 1mm with a 0.2-second measurement time.

Profiles for OAR measurement were obtained at SSDs of 80, 90 and 100cm and depth of 5cm. An adaptive step size was used, with the central 1cm of the field set to 0.2mm, and the outer field set to 0.4mm with a 0.5-second measurement time.

For analysis, the cone data was processed in the BEAMSCAN software by smoothing the individual TMR scans before averaging and normalising in Excel. The OAR data was centred, the step size was re-sampled to 0.25mm before symmetrising the in-plane and cross-plane scans. The average of these processed scans was then also normalised in Excel.

The Varian ICVI Axis Alignment Check was used to confirm the accurate alignment of the cone accessory with respect to the collimator rotation axis on several occasions throughout this investigation. This automated check analyses several images acquired with the portal imaging panel for different collimator angles at gantry 180^0 to ensure the field alignment discrepancy with respect to the collimator rotation axis is no larger than 0.4mm [13].

Output Factor Verification with Radiochromic Film

Verification of the OF measurement was completed using Ashland radiochromic EBT-XD film due to its optimum dose range of 0.4 - 40Gy being best suited to stereotactic clinical applications [14]. Films were exposed in a Standard Imaging solid blue water phantom at 95cm SSD and a depth of 5cm with 10cm of backscatter at gantry 0^0 and collimator 90^0, to match the water tank setup [15]. Film handling, scanning and triple-channel analysis with Ashland's FilmQA Pro software followed the Ashland protocol [16]. Film exposures were scaled to the calibration for the batch of film using reference films which were exposed to known doses under reference conditions with a $10x10cm^2$ field size. All films were scanned using an EPSON Perfection V850 Pro scanner at a resolution of 200dpi and 48bit colour. The time between exposure and scanning was greater than 4 times the interval between the exposure of the reference films and the exposure of the cone films, typically around 2-3 hours, as per Ashland recommendations [16]. No output correction factor was applied to the OF determined by film measurement as radiochromic film is a perturbation-free reference detector (except for volume averaging), as described in TRS-483 [2]. At 200dpi resolution (0.13mm per pixel) the volume averaging effect is negligible.

Verification of Treatment Planning System Dose Calculation Accuracy

After configuring the Eclipse CDC algorithm with the measured OF, TMR and OAR data, a treatment plan was created for a static field defined with the 5mm cone applied to the Standard Imaging phantom mentioned above at 95cm SSD. A coronal dose plane at 5cm depth was created with a size of $7x7cm^2$ and 512x512 pixels, and FilmQA Pro was used to compare this dose plane to the 2D dose distribution resulting from film dosimetry under the same conditions. The two dose distributions were manually registered according to the isodose lines. Triple channel uniformity optimisation was applied for the gamma analysis and the results for each colour channel were averaged to provide a single pass rate. Criteria used for gamma analysis included 1%/1mm to identify any small discrepancies between film dosimetry verification and Eclipse calculation, and 5%/1.5mm which is the criteria used for clinical SRS cases at our institution.

Treatment Planning System Validation Tests

To complete the dose calculation algorithm commissioning checks, end-to-end (E2E) testing was performed using an anthropomorphic head phantom as recommended in AAPM report TG142 for a new or revised procedure [17]. A CIRS 038 Stereotactic End-to-End Verification (STEEV) phantom with the 038-27 single slice film insert was scanned with a clinical stereotactic brain protocol using 1mm slices on a Siemens Somatom Definition AS Open CT scanner [18,19]. The phantom was setup on the CT couch top using a Qfix Encompass SRS insert and customised Qfix Encompass SRS immobilisation mask with headrest.

Contours and library structures were added to the CT image set including the PTV, brain, and patient, as well as the immobilisation equipment and SRS frame. The image set was imported to Eclipse for planning according to clinical SRS planning protocols, with a combination of arc lengths, angles, and directions, as well as couch and collimator angles to test all aspects of the deliverability for this cone aperture size. Three plans were created for this E2E verification to simulate a clinical patient's treatment, one with clockwise arcs on both sides of the head, one with counter-clockwise arcs on the left-hand side only and one with clockwise arcs on the right-hand side only. The patient plan was exported to BrainLab ExacTrac V6.5.2 for treatment preparation as per our clinical SRS treatment workflow [20].

EBT-XD film dosimetry, as described previously, was used for the patient-specific plan QA in accordance with our clinical SRS QA protocol. One film was used per plan. The phantom was set up in the treatment position in line with our cranial SRS treatment protocol, which includes BrainLab ExacTrac x-ray imaging alignment and verification for each couch angle prior to treatment delivery.

Comparison of the film 2D dose distributions and the corresponding Eclipse dose planes was performed as previously described. Fiducial markers inherent to the film insert were used to align the scanned film to the treatment plan. Criteria used for gamma analysis included 1%/1mm, 2%/1mm and 5%/1.5mm to progressively test the limits of the agreement between the film dosimetry results and the Eclipse calculated dose distributions.

Evaluation and Statistical Analysis

Gamma indices for the various comparisons were calculated from the dose difference (DD) and distance to agreement (DTA) of each data point between the two distributions according to equation 1.

$$\Gamma = \sqrt{\left(\frac{DTA}{C_{DTA}}\right)^2 + \left(\frac{DD}{C_{DD}}\right)^2} \qquad (1)$$

Where C_{DTA} is the specified acceptance criterion for DTA in mm and C_{DD} is the specified acceptance criterion for DD in % [21].

This analysis was used for the comparison of TMR and profile data for different measurement techniques and equipment. Comparisons were made between the microDiamond and SRS Diode data, and the microDiamond and GBD for each of the OAR and TMR scans. Gamma analyses for comparisons between film dosimetry results and Eclipse dose plane calculations were carried out in FilmQA Pro, as earlier described.

Results

Results from four iterations of the Varian ICVI Axis Alignment Check over more than two years are shown in table 2 for the 5mm cone. The results for the measurement of TMRs and OARs using the microDiamond and SRS Diode detectors are shown in figures 1-4 while table 3 shows the gamma analysis comparisons between data obtained from the microDiamond and SRS Diode measurements and the GBD. Table 4 shows the measured OFs and comparisons with the GBD and the ACDS audit result. Results for the Eclipse validation tests including OF calculation, dose plane comparison in a solid water phantom, and STEEV plan dose plane comparison are shown in tables 5-6.

Table 2 *– Results from the Varian MPC ICVI Axis Alignment Checks for the 5mm cone.*

Date	5mm cone ICVI alignment to collimator rotation axis (mm)
Check 1	0.18
Check 2: after 0.5 months	0.18
Check 3: after 11 months	0.13
Check 4: after 29 months	0.13

Figure 1 shows the processed, measured microDiamond and SRS Diode TMR data with the GBD overlaid, all normalised to 100%. The standard uncertainty in all measured TMR data is estimated to be 0.5%.

The microDiamond and SRS Diode TMR data were measured in water while the GBD TMRs were measured with a Sun Nuclear Edge Diode in a Gammex 20x20cm^2 solid water phantom [9]. The calculated gamma indices between the microDiamond and SRS Diode data, and microDiamond and GBD are also shown on the plot. It was found that the DTA for the different detector types differed slightly, which may be attributed to their different volume averaging characteristics.

Fig. 1 *– Plot of the normalised and processed measured microDiamond TMR data (in blue) overlaid with the SRS Diode (in orange) and GBD TMRs (in green). Dose percentage is on the primary y-axis, gamma index is on the secondary y-axis and depth in centimetres is on the x-axis. Gamma indices between the microDiamond and SRS Diode data are shown by the dotted orange line and gamma indices between the microDiamond and the GBD are shown by the dotted green line*

Figures 2, 3 and 4 show the processed, measured microDiamond and SRS Diode OAR data at 80cm, 90cm and 100cm SSD respectively, with the GBD overlaid. All profiles are normalised to 100% on the central axis. The standard uncertainty in all measured OAR data is estimated to be 0.5%. OAR data was measured at a 5cm depth in the PTW BEAMSCAN water tank phantom with the microDiamond and SRS Diode, and in an IBA water phantom with a Sun Nuclear Edge Diode for the GBD. The calculated gamma indices between the microDiamond and SRS Diode data, and microDiamond and GBD are also shown on the plots.

Fig. 2 *– Plot of the normalised and processed measured microDiamond 80cm SSD OAR data (in blue) overlaid with the SRS Diode (in orange) and GBD OARs (in green). Dose percentage is on the primary y-axis, gamma index is on the secondary y-axis and off-axis position in millimetres is on the x-axis. Gamma indices between the microDiamond and SRS Diode data are shown by the dotted orange line and gamma indices between the microDiamond and the GBD are shown by the dotted green line*

Fig. 3 *– Plot of the normalised and processed measured microDiamond 90cm SSD OAR data (in blue) overlaid with the SRS Diode (in orange) and GBD OARs (in green). Dose percentage is on the primary y-axis, gamma index is on the secondary y-axis and off-axis position in millimetres is on the x-axis. Gamma indices between the microDiamond and SRS Diode data are shown by the dotted orange line and gamma indices between the microDiamond and the GBD are shown by the dotted green line*

Fig. 4 *– Plot of the normalised and processed measured microDiamond 100cm SSD OAR data (in blue) overlaid with the SRS Diode (in orange) and GBD OARs (in green). Dose percentage is on the primary y-axis, gamma index is on the secondary y-axis and off-axis position in millimetres is on the x-axis. Gamma indices between the microDiamond and SRS Diode data are shown by the dotted orange line and gamma indices between the microDiamond and the GBD are shown by the dotted green line*

Table 3 shows the gamma analysis pass rates between the microDiamond and SRS Diode measured TMRs and OARs, and the microDiamond and GBD TMRs and OARs. The gamma pass rates were calculated using equation 1 with a criterion of 1%/1mm. The uncertainties for the gamma pass rates were calculated as the averaged standard deviation at different off-axis positions for the OARs and depths for the TMRs. The OARs are reported based on the SSD they were measured at, all at a depth of 5cm.

Table 3 *– Gamma analysis pass rates for 1%/1mm criterion between microDiamond and SRS Diode TMRs and 80, 90 and 100cm SSD OARs with associated uncertainties, and gamma analysis pass rates for 1%/1mm criterion between microDiamond and GBD TMRs and 80, 90 and 100cm SSD OARs with associated uncertainties.*

MicroDiamond	SRS Diode Gamma	GBD Gamma
TMR	99.31 ± 1%	98.91 ± 2%
80cm SSD OAR	96.58 ± 3%	95.96 ± 4%
90cm SSD OAR	97.05 ± 2%	96.56 ± 5%
100cm SSD OAR	97.45 ± 2%	96.41 ± 5%

Table 4 shows the measured OF and FWHMs for the microDiamond and SRS Diode, values from the Varian GBD, the OF measured by the ACDS during the Level 1b small field audit carried out during linac commissioning using their PTW 60019 microDiamond, and the EBT-XD film measured OF. The uncertainties for the microDiamond and SRS Diode measured OFs are tabulated as expanded uncertainties with k=2. The FWHMs were calculated for the three measured OARs at 80cm, 90cm and 100cm SSDs, at a depth of 5cm. The nominal diameter at depth based on SSD are also shown, which were used as a reference for estimating the errors in the measured FWHMs. The standard uncertainty for the microDiamond measured OF was calculated by adding in quadrature the electrometer readings for the two dose rates for the cone dose and 10x10cm^2 field dose assumed

to have a measurement uncertainty of 0.5%, and the TRS-483 published uncertainty for the field output correction factor of 0.8% [2]. The standard uncertainty for the SRS Diode measured OF was calculated by adding in quadrature the electrometer readings for the cone dose, 10x10cm^2 field dose and intermediate field size dose used for daisy chaining assumed to have a measurement uncertainty of 0.5%, as well as the TRS-483 published uncertainty for the field output correction factor of 0.8% [2]. The uncertainties in the doses obtained from the cone and 10x10cm^2 field films were calculated using the average standard deviation for the three colour channels, which were added in quadrature to determine the uncertainty in the resulting OF, rounded up to the nearest integer.

Table 4 *– MicroDiamond and SRS Diode measured OFs and FWHMs for 3 measured OARs at 80, 90 and 100cm SSDs at a depth of 5cm with associated uncertainties, GBD output ratio and FWHMs for OARs at 80, 90 and 100cm SSDs at a depth of 5cm, nominal diameter at depth based on SSD, ACDS measured OF, and EBT-XD film measured OF with associated uncertainty.*

Measured	**OF**	**FWHM D5 (mm)**		
		80SSD	**90SSD**	**100SSD**
MicroDiamond	0.623 ± 0.014	4.04 ± 5%	4.52 ± 5%	5.00 ± 5%
SRS Diode	0.631± 0.016	4.09 ± 4%	4.56 ± 4%	5.05 ± 4%
Varian GBD	0.664 (output ratio)	3.99 ± 5%	4.29 ± 5%	4.69 ± 5%
Nominal diameter at depth	-	4.25	4.75	5.25
ACDS	0.625	-	-	-
EBT-XD	0.631 ± 1%	-	-	-

From the results and analysis above, it was decided to configure the CDC algorithm in Eclipse for the 5mm cone with the TMRs and OARs measured with the SRS Diode, and the OF measured with the microDiamond. This was due to the decreased volume averaging evident in the profile measurements with the SRS Diode compared to the microDiamond measurements, and the greater confidence in the microDiamond small field output correction factor. To ensure the Eclipse TPS was correctly using this newly entered measured data, OFs calculated in Eclipse were compared to these measurements and 5mm cone dose planes from Eclipse were compared to EBT-XD film measurements using gamma analysis.

Table 5 shows the Eclipse calculated OFs using the microDiamond data for 0.5mm and 1mm calculation grid sizes in the TPS cone planning module at 95cm SSD and depth of 5cm with 10cm of backscatter. To further show the effect of the calculation grid size on the resulting OF values, the isocentre was shifted in-plane and cross-plane by half the grid size. This resulted in an additional difference in the determined OFs for the 0.5mm and the 1mm calculation grid sizes of 0.7% and -3.2%, respectively. To test whether the OF determined in Eclipse could be more consistent with the microDiamond measurement, a 50x50x50cm^3 water equivalent phantom was also modelled in the TPS for the collection of the cone dose and 10x10cm^2 reference dose for the OF calculation. Differences between the Eclipse calculated OFs and the microDiamond measured OF are also shown in the table.

Table 5 *– Eclipse calculated OFs using 0.5 and 1mm calculation grid sizes with differences from the microDiamond OF (% Diff to MD), and Eclipse calculated OFs using the offset solid water and 50x50x50cm^3 modelled phantom using 0.5 and 1mm calculation grid sizes with differences from the microDiamond OF.*

Phantom	**0.5mm Calc grid size**		**1mm Calc grid size**	
	OF	**% Diff to MD**	**OF**	**% Diff to MD**
Solid water	0.609	-2.2	0.618	-0.8
Solid water offset isocentre	0.613	-1.6	0.598	-4.0
50x50x50cm^3 Water equivalent phantom	0.610	-2.1	0.605	-2.9

Table 6 shows the FilmQA Pro gamma analysis pass rates for criterion of 1%1mm and 5%/1.5mm for the OF dose plane, and gamma analysis pass rates for criterion of 1%1mm, 2%/1mm and 5%/1.5mm for dose planes from each field in the STEEV patient-specific QA plan measured with EBT-XD film. The uncertainties for the pass rates were calculated using the standard deviation of pass rates between the colour channels in the optimisation.

Table 6 *– FilmQA Pro gamma analysis pass rates for criterion of 1%/1mm, and 5%/1.5mm for the OF dose plane, and gamma analysis pass rates for criterion of 1%/1mm, 2%/1mm and 5%/1.5mm for the STEEV patient-specific QA plan using EBT-XD film, with associated uncertainties.*

Plan	**FilmQA Pro Result**		
	1%/1mm	**2%/1mm**	**5%/1.5mm**

OF	99.2 ± 0.2%	-	100%
6.1 – CCW LHS	92.07 ± 0.2%	97.99 ± 0.4%	100%
6.2 – CW L&R	97.99 ± 0.2%	99.93 ± 0.03%	100%
6.3 – CW RHS	97.85 ± 0.2%	99.98 ± 0.01%	100%

Discussion

Conical collimators accurately define very small linac radiation fields suitable for stereotactic radiosurgery of regularly shaped cranial targets, surpassing the accuracy of field definition achievable with multi-leaf collimators. Table 2 shows that the alignment of our 5mm cone collimator with respect to the collimator rotation axis was consistently better than 0.2mm over a period of almost 2.5 years.

Measurements to characterise such very small radiation fields, particularly output factors, are notoriously difficult and prone to error. ARPANSA have reported a significant variation of measured output factors with a standard deviation of 3.6% between measurements during a comparison exercise with a single linac at their centre. The measurements involved several different detector types, correction factors, setup variations, and analysis methods, highlighting the importance of completing accurate measurements with suitable detectors as well as obtaining or deriving appropriate correction factors [5].

Consistency between measurements performed with different detectors is essential to achieving confidence in results. This study, which included output factor measurements for a Varian 5mm circular collimator using three different detectors, as well as comparisons with an independent ACDS audit and with the Varian Golden Beam Data, showed good consistency between the various results apart from the uncorrected GBD output ratio. Comparisons with the GBD were considered valid since the linac had been beam-matched to it, and the GBD is an average dataset representing multiple beam-matched TrueBeam linacs.

The OF measured with our microDiamond detector agrees well with the ACDS measured OF using their microDiamond detector of the same type, with the small discrepancy being most likely due to the application of slightly different user-defined correction factors (within 0.2%). Given the difficulty of measurement and the good agreement between these OFs, this reproducibility provides confidence in our measurement technique. The output ratio provided in the GBD was published before the TRS-483 protocol became available. It was later reported by Varian that the GBD output factors did not include a small field correction factor, accounting for the difference from the measured OF from this investigation [2,9]. Applying the Edge detector correction factor (0.942) for the 5mm cone used by Cheng et al (2016) to the GBD output ratio results in an OF of 0.625, very close to our microDiamond and the ACDS microDiamond measured results [3].

Cheng et al (2016) reported Monte Carlo (MC)-simulated and measured OFs for the same equipment and parameters (Varian TrueBeam 6FFF modality, 95cm SSD and 5cm measurement depth) applicable to this investigation, therefore their results are potentially useful for comparison purposes although their reported OFs are referenced to a 5x5cm^2 field rather than a 10x10cm^2 field. Small field correction factors were applied to their measured output ratios; however, their work was carried out before the publication of the TRS-483 protocol and therefore different sources were used for these factors. Their OF results, after renormalising to a 10x10cm^2 reference field using a measured 5x5cm^2 OF of 0.938 (compared to 0.940 from the GBD), were 0.629 for an Edge detector measurement, 0.617 from a measurement with an IBA SFD detector, and 0.632 for a MC simulation using a 0.25 mm^3 voxel size [3].

The overall good consistency between our microDiamond measured OF and the available comparison data from the literature provided further confidence in our result. There was a preference to settle on a measured OF based on a small field correction factor covered in TRS-483 without the need for extrapolation, notwithstanding potential correction factor dependencies unaccounted for according to work by Casar et al (2018) such as differences in linac vendor and configuration, beam energy, and collimation type [22]. Our SRS Diode measured OF was also consistent with the available comparison data and with our microDiamond measured OF, however it relied on unpublished data for derivation of the correction factor in TRS-483, and it required the intermediate field size daisy chaining method due to the field size limitations for the detector, potentially adding to the uncertainty of this result. For these reasons the microDiamond measured OF was preferred for the Eclipse algorithm configuration. The range of OFs from the six different measurement methods discussed here (microDiamond, SRS Diode, Edge, EBT-XD, SFD and MC) suggests that the real value for the 5mm cone OF is approximately 0.625 ± 0.015. This value agrees well with our microDiamond and SRS Diode measured OFs within the expanded uncertainties reported in table 4.

It was noted that there was a consistent 0.2mm difference between the nominal diameter at depth and measured values, however this had a negligible (~0.1% difference) effect on the resulting correction factors for both detectors used in this investigation.

There was generally good agreement between the TMR and OAR data measured with the microDiamond and SRS Diode detectors, and with the GBD. As expected, some variations were observed between the OAR data

sets off-axis due to the differences in volume averaging effects for different size detectors. The slightly increased volume averaging effect evident in the microDiamond profiles led to the decision to configure the Eclipse CDC algorithm with the SRS Diode TMR and OAR data. Although the microDiamond has a smaller nominal sensitive volume of 0.004mm^3 compared to the SRS Diode's sensitive volume of 0.3mm^3, it has a larger entrance window radius of 1.1mm compared to the 0.6mm radius of the SRS Diode. This leads to more volume averaging in a plane perpendicular to the radiation beam axis, even though both detectors have identical outer dimensions [6]. The GBD OARs differ from the microDiamond measured OAR data more than the SRS Diode measured OARs do, as evidenced by Figures 2 – 4 and the corresponding gamma analysis results in Table 3. This is consistent with different volume averaging effects for the three detectors, since the Edge detector has an even smaller sensitive volume in a plane perpendicular to the beam axis (0.8 x 0.8mm) [23]. There may also be variations caused by different measurement techniques, for example the use of different step sizes for OAR data collection. The GBD were measured with a 1mm step size and resampled to 0.25mm increments while the microDiamond and SRS Diode data were collected with a smaller variable step size across the profile and resampled to 0.25mm.

As shown in Table 5, the Eclipse calculated OF was consistently underestimated compared to the measured OF, both for calculation in a solid water phantom and in a 50x50x50cm^3 water volume representing the geometry of the water tank phantom used for the measurements. The reasons for this are unclear, although one contributing factor could be the way Eclipse generates TMRs from the input measured data. The CDC configuration program generates adapted TMR data, interpolates it linearly up to 10mm and then models that data with an equation, which could be associated with errors in the model [12]. We found that for the 5mm cone the difference between the processed measured TMR data and the Eclipse calculated TMR at a depth of 5cm was 1%. Despite this OF discrepancy, the film dosimetry comparison with an Eclipse calculated dose plane in solid water at 5cm depth demonstrated good agreement on gamma analysis (Table 6).

Table 5 shows a significant dependence on field placement in Eclipse for the 1mm grid size calculation. A 0.5mm offset of the isocentre within the fixed calculation grid introduced a change in the calculated OF of more than 3%. This was not evident with a 0.5mm calculation grid, highlighting the importance of fine resolution for very small field calculations with Eclipse.

The end-to-end measurements in the anthropomorphic STEEV phantom, simulating the patient journey through an SRS treatment including simulation, contouring, planning, treatment, and QA, did not reveal any issues in the clinical process or dose calculation for the 5mm cone. Films were analysed with the clinical tolerance of 5%/1.5mm as well as tighter specifications of 2%/1mm and 1%/1mm to test the limits of the agreement between the delivery and the plan. All plans achieved a 95% pass rate for the tightest analysis criteria apart from the counter-clockwise plan having a lower pass rate of 92%. Optimal pass rates of 100% were obtained for all plans using the clinical tolerance, demonstrating confidence in patient treatment with the 5mm cone.

Uncertainties in this investigation include the measurement uncertainties for the cone and reference fields, measurement uncertainties of the TMRs and OARs using the microDiamond and SRS Diode detectors, gamma analysis pass rate uncertainties, uncertainties related to the Eclipse calculation algorithm and data modelling, and uncertainty in the small field output correction factors. Type A uncertainties were minimised by ensuring sufficient measurements were made to allow appropriate statistical analysis. Type B uncertainties were reduced with the use of appropriate equipment following extensive literature review, optimising measurement procedures and estimation of associated uncertainties using trusted literature to calculate the error in measured values to best represent the quality of the experimental data.

Conclusion

The CDC algorithm of our Eclipse TPS was successfully configured for the 5mm ICVI cone accessory attached to a Varian TrueBeam accelerator at energy 6FFF using an OF measured with a microDiamond detector, and TMR and OAR data measured with an SRS Diode detector. Validation of this data and TPS performance testing included comparisons with the Varian GBD, an independent ACDS measured OF, and radiochromic film measurements, followed by end-to-end testing with radiochromic film dosimetry in an anthropomorphic phantom.

Declarations

Funding: no funding was received for conducting this study.
Conflict of interest: all authors declare that they have no conflicts of interest.
Ethical approval: this article does not contain any studies with human participants performed by any of the authors.

Acknowledgements The authors would like to thank Emma Spelleken for advice on film techniques, and Lockie Yuen for guidance on gamma analysis for this study.

Reference list

[1] International Commission on Radiation Units and Measurements (2014) Journal of the ICRU Volume 14 No. 2 2014: ICRU Report 91 Prescribing, Recording, and Reporting of Stereotactic Treatments with Small Photon Beams. Oxford University Press: Oxford.

[2] International Atomic Energy Agency (2017) Technical Report Series No. 483 Dosimetry of Small Static Fields Used in External Beam Radiotherapy: An International Code of Practise for Reference and Relative Dose Determination. IAEA: Vienna.

[3] Cheng JY, Ning H, Arora BC, Zhuge Y, Miller RW (2016) Output factor comparison of Monte Carlo and measurement for Varian TrueBeam 6 MV and 10 MV flattening filter-free stereotactic radiosurgery system. J App Clin Med Phys **17**(3):pp100-110.

[4] Smith CL, Montesari A, Oliver CP, Butler DJ (2019) Evaluation of the IAEA-TRS 483 protocol for the dosimetry of small fields (square and stereotactic cones) using multiple detectors. J App Clin Med Phys **21**(2):pp98-110.

[5] Oliver CP, Butler DJ, Takau V, Williams I (2017) Survey of 5 mm small-field output factor measurements in Australia. J App Clin Med Phys **19**(2):pp329-337.

[6] Physikalisch-Technische Werkstatten (2017) Small Field Dosimetry Application Guide. PTW: Freiburg.

[7] Physikalisch-Technische Werkstatten (2019) PTW Beamscan. PTW dosimetry. http://www.ptwdosimetry.com. Accessed 26 March 2022

[8] Underwood TSA, Rowland BC, Ferrand R, Vieillevigne L (2015) Application of the Extradin W1 scintillator to determine Ediode 60017 and microDiamond 60019 correction factors for relative dosimetry within small MV and FFF fields. Phys Med Bio **60**(1):pp6669-6683.

[9] Varian Medical Systems (2020) ICVI Conical Collimators Representative Beam Data for Eclipse. Varian. http://www.myvarian.com. Accessed 26 March 2022

[10] Kairn T, Charles PH, Cranmer-Sargison G, Crowe SB, Langton CM, Thwaites DI, Trapp JV (2015) Clinical use of diodes and micro-chambers to obtain accurate small field output factor measurements. Australas Phys Eng Sci Med **38**(1):pp357-367.

[11] Das IJ, Francescon P, Moran JM, Ahnesjo A, Aspradakis MM, Cheng C, Ding GX, Fenwick JD, Huq MS, Oldham M, Reft CS, Sauer OA (2021) Report of AAPM Task Group 155: Megavoltage photon beam dosimetry in small fields and non-equilibrium conditions. Med Phys **48**:ppe886-e921.

[12] Varian Medical Systems (2017) Eclipse Photon and Electron Algorithms Reference Guide. Varian: California.

[13] Varian Medical Systems (2008) TrueBeam / TrueBeam STx / Edge / VitalBeam Software v2.x: Installation Product Acceptance. Varian: California.

[14] Ashland (2020) Gafchromic Dosimetry Media, Type EBT-XD. Ashland. http://www.gafchromic.com. Accessed 26 March 2022

[15] Standard Imaging (2020) Blue Water Phantom. Standard Imaging. http://www.standardimaging.com. Accessed 26 March 2022

[16] Ashland (2021) Efficient Protocols for Accurate Radiochromic Film Calibration and Dosimetry. Ashland. http://www.gafchromic.com. Accessed 26 March 2022

[17] Klein EE, Hanley J, Bayouth J, Yin F, Simon W, Dresser S, Serago C, Aguirre F, Ma L, Arjomandy B, Liu C (2009) Task Group 142 report: Quality assurance of medical accelerators. Med Phys **36**(9):pp4197-4212.

[18] CIRS Tissue Simulation & Phantom Technology (2013) Phantom Patient for Stereotactic End-to-End Verification Model 038 STEEV. CIRS inc. http://www.cirsinc.com. Accessed 26 March 2022

[19] Siemens (2013) Siemens Somatom Definition AS. Siemens Healthineers. http://siemens-healthineers.com. Accessed 26 March 2022

[20] BrainLab (2017) BrainLab ExacTrac Version 6.5. BrainLab. http://www.brainlab.com. Accessed 26 March 2022

[21] Low DA, Harms WB, Mutic S, Purdy JA (1998) A technique for the quantitative evaluation of dose distributions. Med Phys **25**(5):pp656-661.

[22] Casar B, Gershkevitsh E, Mendez I, Jurkovic S, Huq MS (2018) A novel method for the determination of field output factors and output correction factors for small static fields for six diodes and a microdiamond detector in megavoltage photon beams. Med Phys **46**(2):pp944-963.

[23] Sun Nuclear (2020) Edge Detector. Sun Nuclear. http://www.sunnuclear.com. Accessed 26 March 2022

Figures

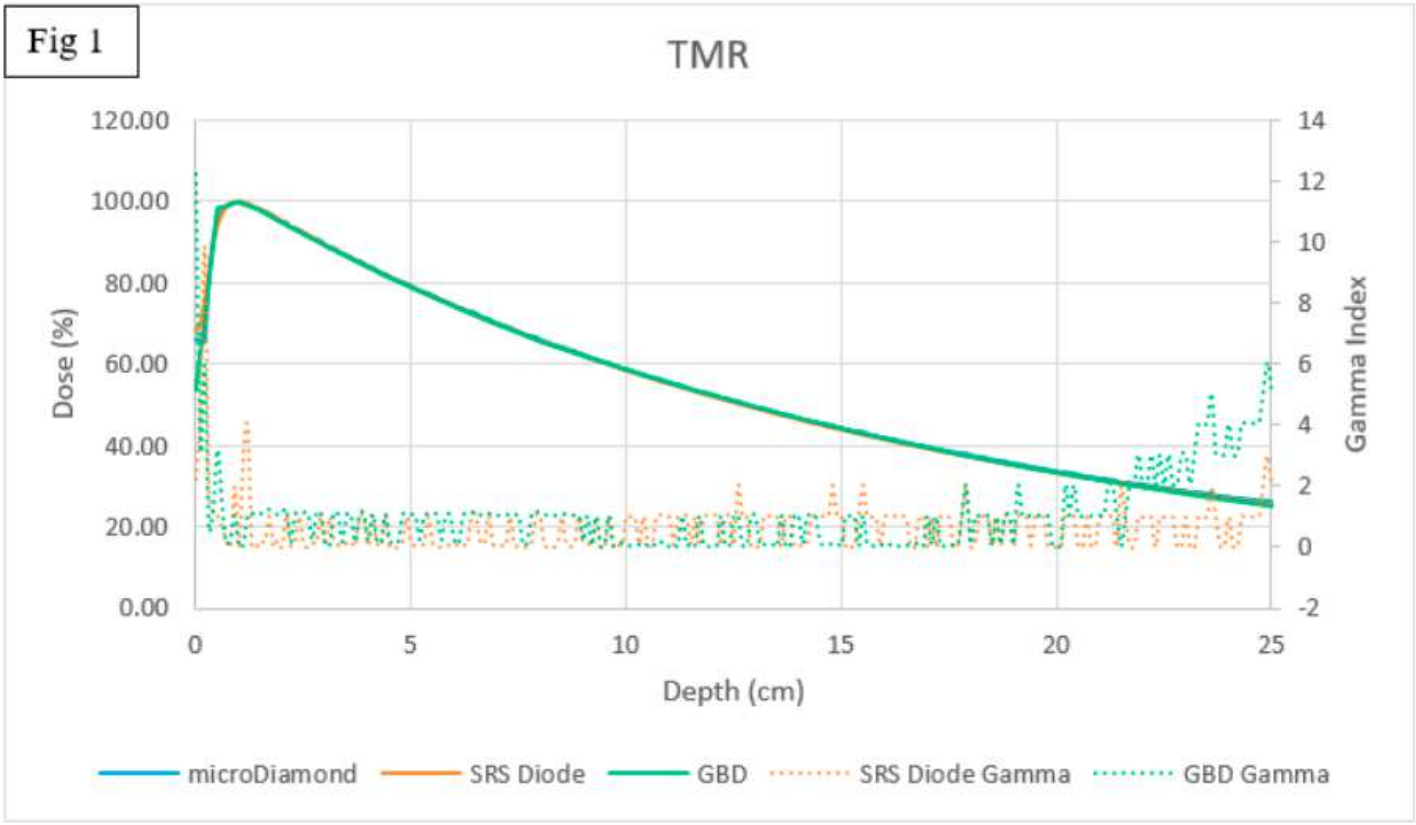

Figure 1

Plot of the normalised and processed measured microDiamond TMR data (in blue) overlaid with the SRS Diode (in orange) and GBD TMRs (in green). Dose percentage is on the primary y-axis, gamma index is on the secondary y-axis and depth in centimetres is on the x-axis. Gamma indices between the microDiamond and SRS Diode data are shown by the dotted orange line and gamma indices between the microDiamond and the GBD are shown by the dotted green line

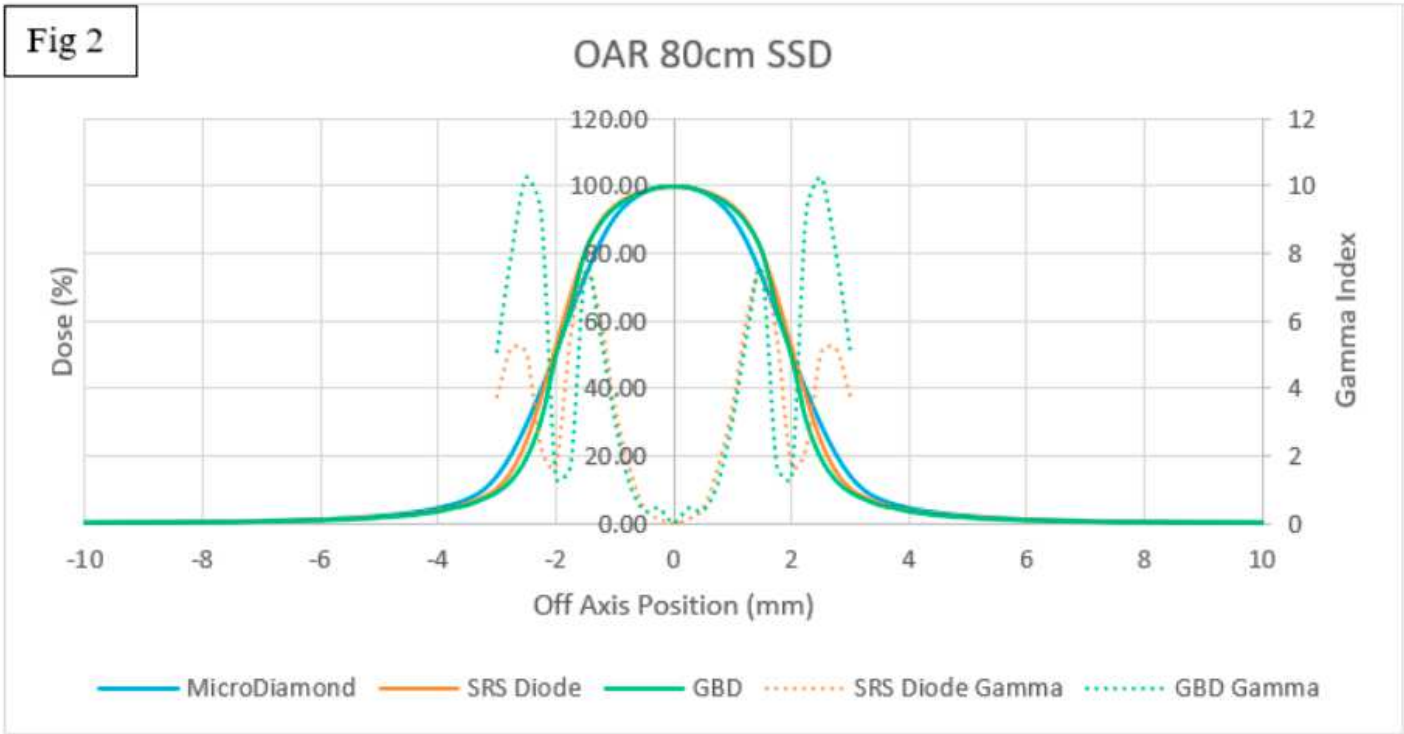

Figure 2

Plot of the normalised and processed measured microDiamond 80cm SSD OAR data (in blue) overlaid with the SRS Diode (in orange) and GBD OARs (in green). Dose percentage is on the primary y-axis, gamma index is on the secondary y-axis and off-axis position in millimetres is on the x-axis. Gamma indices between the microDiamond and SRS Diode data are shown by the dotted orange line and gamma indices between the microDiamond and the GBD are shown by the dotted green line

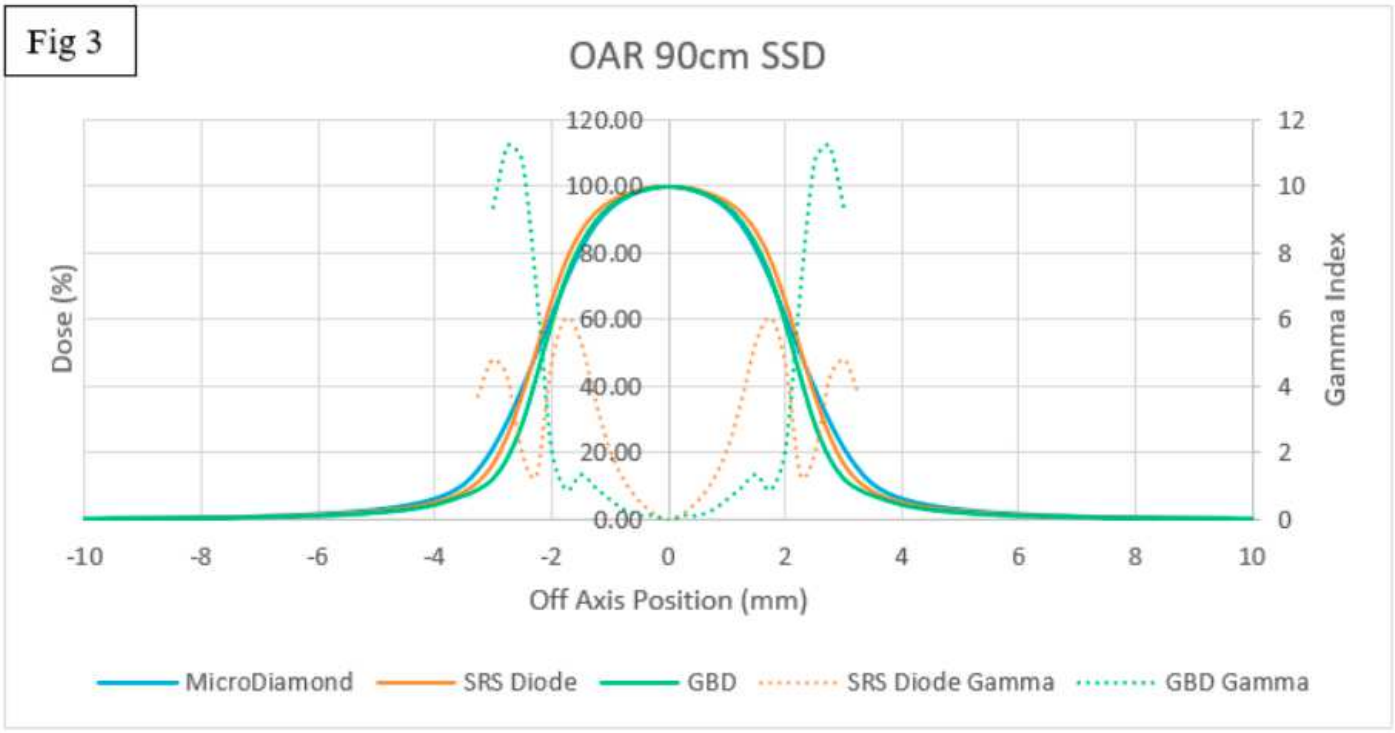

Figure 3

Plot of the normalised and processed measured microDiamond 90cm SSD OAR data (in blue) overlaid with the SRS Diode (in orange) and GBD OARs (in green). Dose percentage is on the primary y-axis, gamma index is on the secondary y-axis and off-axis position in millimetres is on the x-axis. Gamma indices between the microDiamond and SRS Diode data are shown by the dotted orange line and gamma indices between the microDiamond and the GBD are shown by the dotted green line

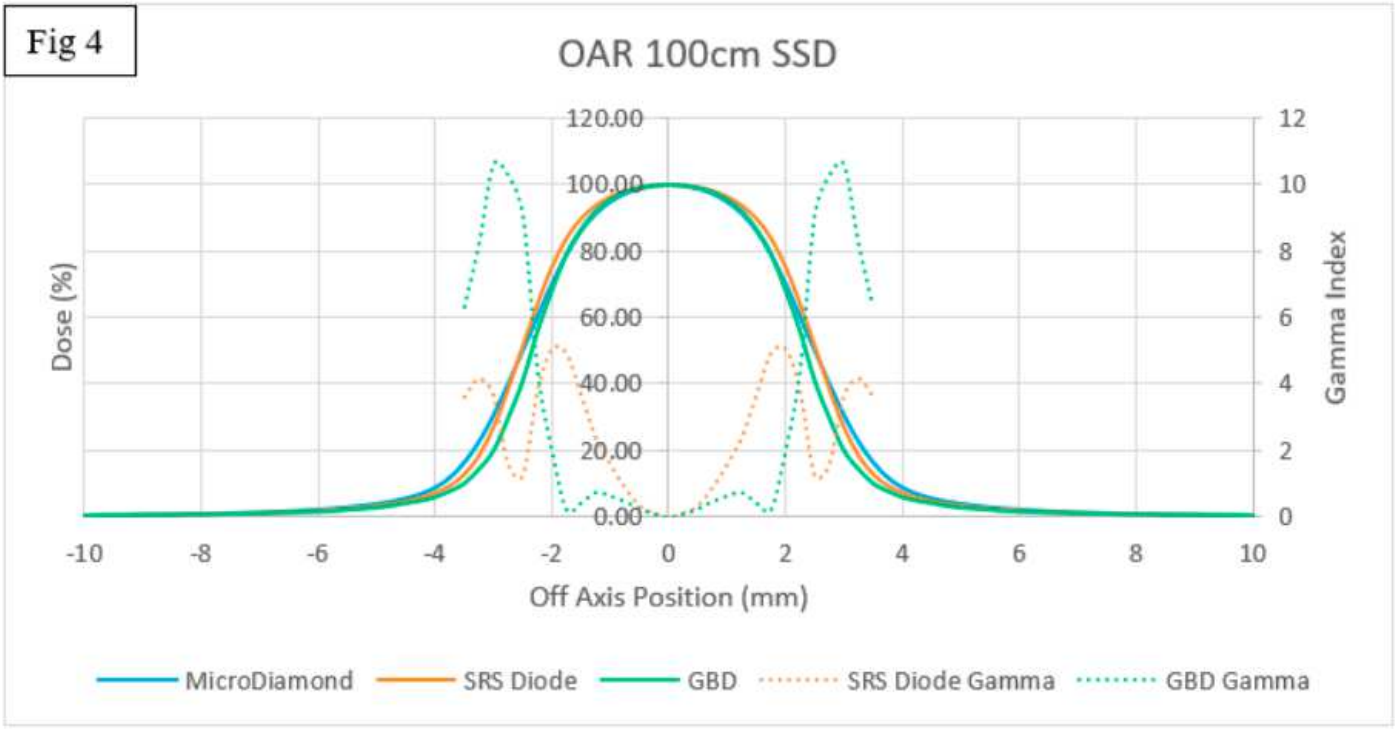

Figure 4

Plot of the normalised and processed measured microDiamond 100cm SSD OAR data (in blue) overlaid with the SRS Diode (in orange) and GBD OARs (in green). Dose percentage is on the primary y-axis, gamma index is on the secondary y-axis and off-axis position in millimetres is on the x-axis. Gamma indices between the microDiamond and SRS Diode data are shown by the dotted orange line and gamma indices between the microDiamond and the GBD are shown by the dotted green line